Hindawi Publishing Corporation
EURASIP Journal on Advances in Signal Processing
Volume 2010, Article ID 181403, 9 pages
doi:10.1155/2010/181403

Research Article

Particle Filtering: The Need for Speed

Gustaf Hendeby,[1] Rickard Karlsson,[2] and Fredrik Gustafsson (EURASIP Member)[3]

[1] *Department of Augmented Vision, German Research Center for Artificial Intelligence, 67663 Kaiserslatern, Germany*
[2] *NIRA Dynamics AB, Teknikringen 6, 58330 Linköping, Sweden*
[3] *Department of Electrical Engineering, Linköping University, 58183 Linköping, Sweden*

Correspondence should be addressed to Rickard Karlsson, rickard@isy.liu.se

Received 22 February 2010; Accepted 26 May 2010

Academic Editor: Abdelak Zoubir

The *particle filter* (PF) has during the last decade been proposed for a wide range of localization and tracking applications. There is a general need in such embedded system to have a platform for efficient and scalable implementation of the PF. One such platform is the *graphics processing unit* (GPU), originally aimed to be used for fast rendering of graphics. To achieve this, GPUs are equipped with a parallel architecture which can be exploited for *general-purpose computing* on GPU (GPGPU) as a complement to the central processing unit (CPU). In this paper, GPGPU techniques are used to make a parallel recursive Bayesian estimation implementation using particle filters. The modifications made to obtain a parallel particle filter, especially for the resampling step, are discussed and the performance of the resulting GPU implementation is compared to the one achieved with a traditional CPU implementation. The comparison is made using a minimal sensor network with bearings-only sensors. The resulting GPU filter, which is the first complete GPU implementation of a PF published to this date, is faster than the CPU filter when many particles are used, maintaining the same accuracy. The parallelization utilizes ideas that can be applicable for other applications.

1. Introduction

The signal processing community has for a long time been relying on Moore's law, which in short says that the computer capacity doubles for each 18 months. This technological evolution has been possible by down-scaling electronics where the number of transistors has doubled every 18 months, which in turn has enabled more sophisticated instructions and an increase in clock frequency. The industry has now reached a phase where the power and heating problems have become limiting factors. The increase in processing speed of the CPU (*central processing unit*) has been exponential since the first microprocessor was introduced in 1971 and in total it has increased one million times since then. However, this trend stalled a couple of years ago. The new trend is to double the number of cores in CMP (*chip multicore processing*), and the number of cores is expected to follow Moore's law for the next ten years [1]. The software community is now looking for new programming tools to utilize the parallelism of CMPs, which is not an easy task [2]. The signal processing community has also started to focus more on distributed and parallel implementations of the core algorithms.

In this contribution, the focus is on distributed *particle filter* (PF) implementations. The particle filter has since its introduction in its modern form [3] turned into a standard algorithm for nonlinear filtering, and is thus a working horse in many current and future applications. The particle filter is sometimes believed to be trivially parallelizable, since each core can be responsible for the operations associated with one or more particles. This is true for the most characteristic steps in the PF algorithm applied to each particle, but not for the interaction steps. Further, as is perhaps less well known, the bottle neck computation even on CPU's is often not the particle operations but the resampling [4], and this is not obvious to parallelize, but possible.

The main steps in the PF and their complexity as a function of the number N of particles are summarized below, and all details are given in Section 3.

(i) Initialization: each particle is sampled from a given initial distribution and the weights are initialized to a constant; parallelizable and thus $\mathcal{O}(1)$.

(ii) Measurement update: the likelihood of the observation is computed conditional on the particle; parallelizable and thus $\mathcal{O}(1)$.

(iii) Weight normalization: the sum of the weight is needed for normalization. A hierarchical evaluation of the sum is possible, which leads to complexity $\mathcal{O}(\log(N))$.

(iv) Estimation: the weighted mean is computed. This requires interaction. Again, a hierarchical sum evaluation leads to complexity $\mathcal{O}(\log(N))$.

(v) Resampling: this step first requires explicitly or implicitly a *cumulative distribution function* (CDF) to be computed from the weights. There are different ways to solve this, but it is not obvious how to parallelize it. It is possible to make this a $\mathcal{O}(\log(N))$ operation. There are other interaction steps here commented on in more detail later on.

(vi) Prediction: each particle is propagated through a common proposal density, parallelizable and thus $\mathcal{O}(1)$.

(vii) Optional steps of Rao-Blackwellization: if the model has a linear Gaussian substructure, part of the state vector can be updated with the Kalman filter. This is done locally for each particle, and thus $\mathcal{O}(1)$.

(viii) Optional step of computing marginal distribution of the state (the filter solution) rather than the state trajectory distribution. This is $\mathcal{O}(N^2)$ on a single core processor, but parallelizable to $\mathcal{O}(N)$. It also requires massive communication between the particles.

This suggests the following basic functions of complexity for the extreme cases single core, $M = 1$, and complete parallelization, $M/N \to 1$:

$$\begin{aligned}\text{Single-core}: f_1(N) &= c_1 + c_2 N,\\ \text{Multicore}\left(\frac{M}{N} \longrightarrow 1\right): f_M(N) &= c_3 + c_4 \log(N).\end{aligned} \tag{1}$$

For a fixed number of particles and sufficiently large number of cores the parallel implementation will always be more efficient. In the future, we might be able to use $N = M$. However, for the N that the application requires, the best solution depends on the constants. One can here define a break-even number

$$\overline{N} = \underset{N}{\text{sol}}\{f_1(N) = f_M(N)\}. \tag{2}$$

This number depends on the relative processing speed of the single and multicore processors, but also on how efficient the implementation is.

It is the purpose of this contribution to discuss these important issues in more detail, with a focus on *general purpose graphical processing units* (GPGPUs). We also provide the first complete GPGPU implementations of the PF, and use this example as a ground for a discussion of $\overline{N}$.

Multicore implementations of the PF has only recently been studied. For instance, [5] presents a GPU PF for visual 2d tracking, [6] focusing on doing parallel resampling on a FPGA, and [7, 8] relating to this work. To the best of the authors' knowledge no successful complete implementation of a general PF algorithm on a GPU has previously been reported.

The organization is as follows. Since parallel programming may be unfamiliar to many researchers in the signal processing community, we start with a brief tutorial in Section 2, where background material for parallel programming, particularly using the graphics card, is reviewed. In Section 3 recursive Bayesian estimation utilizing the particle filter is presented for a GPU implementation. In Section 4 a simulation study is presented comparing CPU and GPU performance. Finally, Section 5 summarizes the results.

Table 1: Table describing how the number of pipelines in the GPU has changed. (The latest generation of graphics cards form the two main manufacturers, NVIDIA, and ATI, have unified shaders instead of specialized ones. These are marked with †.)

Model	Vertex pipes	Frag. pipes	Year
NVIDIA GeForce 6800 Ultra	6	16	2004
ATI Radeon X850 XT PE	6	16	2005
NVIDIA Geforce 7900 GTX	8	24	2006
NVIDIA Geforce 7950 GX2	16	48	2006
ATI Radeon X1900 XTX	8	48	2006
NVIDIA GeForce 8800 Ultra	$128^\dagger$	$128^\dagger$	2007
ATI Radeon HD 2900 XT	$320^\dagger$	$320^\dagger$	2007
NVIDIA GeForce 9800 GTX+	$128^\dagger$	$128^\dagger$	2008
ATI Radeon HD 4870 X2	$2 \times 800^\dagger$	$2 \times 800^\dagger$	2008
NVIDIA GeForce 9800 GT2	$2 \times 128^\dagger$	$2 \times 128^\dagger$	2008
NVIDIA GeForce 295 GTX	$2 \times 240^\dagger$	$2 \times 240^\dagger$	2009
ATI Radeon HD 5870	$1600^\dagger$	$1600^\dagger$	2009
NVIDIA GeForce 380 GTX	$512^\dagger$	$512^\dagger$	2009

2. Parallel Programming

Nowadays, there are many types of parallel hardware available; examples include multicore processors, *field-programmable gate arrays* (FPGAs), computer clusters, and GPUs. GPUs offer low-cost and easily accessible *single instruction multiple data* (SIMD) parallel hardware—almost every new computer comes with a decent graphics card. Hence, GPUs are an interesting option not only for speeding up algorithms but also for testing parallel implementations.

The GPU architecture is also attractive since there is a lot of development going on in this area, and support structures are being implemented. One example of this is *Matrix Algebra on* GPU *and Multicore Architectures* (MAGMAs), [9], which brings the functionality of LAPACK to the GPU. There are also many success stories, where CUDA implementations of various algorithms have proved several times faster than normal implementations [10].

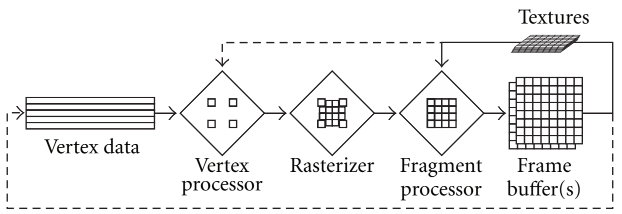

Figure 1: The graphics pipeline. The vertex and fragment processors can be programmed with user code which will be evaluated in parallel on several pipelines. In the latest GPUs these shaders are unified instead of specialized as depicted.

2.1. Graphics Hardware. Graphics cards are designed to primarily produce graphics, which makes their design different from general purpose hardware, such as the CPU. One such difference is that GPUs are designed to handle huge amounts of data about an often complex scene in real time. To achieve this, the GPU is equipped with a SIMD parallel instruction set architecture. The GPU is designed around the standardized graphics pipeline [11] depicted in Figure 1. It consists of three processing steps, which all have their own purpose when it comes to producing graphics, and some dedicated memory units. From having predetermined functionality, GPUs have moved towards providing more freedom for the programmer. Graphics cards allow for customized code in two out of the three computational units: the vertex shader and the fragment shader (these two steps can also be unified in one shader). As a side-effect, *general-purpose computing on graphics processing units* (GPGPUs) has emerged to utilize this new source of computational power [11–13]. For highly parallelizable algorithms the GPU may outperform the sequential CPU.

2.2. Programming the GPU. The two programmable steps in the graphics pipeline are the vertex processor and the fragment processor, or if these are unified. Both these processors can be controlled with programs called *shaders*. Shaders, or GPU programs, were introduced to replace fixed functionality in the graphics pipeline with more flexible programmable processors.

Some prominent differences between regular programming and GPU programming are the basic data types which are available, colors and textures. In newer generations of GPUs 32 bit floating point operations are supported, but the rounding units do not fully conform to the IEEE floating point standard, hence providing somewhat poorer numerical accuracy. Internally the GPU works with quadruples of floating point numbers that represent colors (red, green, blue, and alpha) and data is passed to the GPU as *textures*. Textures are intended to be pictures that are mapped onto surfaces given by the vertices.

In order to use the GPU for general purpose calculations, a typical GPGPU application has a program structure similar to Figure 2.

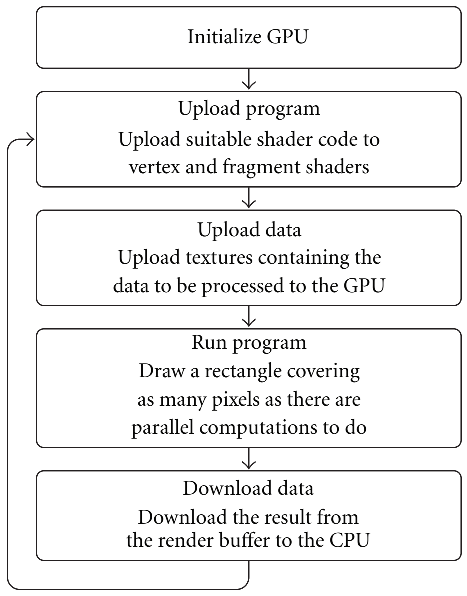
Initialize GPU
Upload program
Upload suitable shader code to vertex and fragment shaders
Upload data
Upload textures containing the data to be processed to the GPU
Run program
Draw a rectangle covering as many pixels as there are parallel computations to do
Download data
Download the result from the render buffer to the CPU

Figure 2: Work flow for GPGPU programming using the *OpenGL shading language* (GLSL).

2.3. GPU Programming Language. There are various ways to access the GPU resources as a programmer. Some of the available alternatives are

(i) OpenGL [14] using the *OpenGL Shading Language* (GLSL) [15],

(ii) *C for graphics* (Cg) [16],

(iii) DirectX High-Level Shader Language (HLSL) [17],

(iv) CUDA [18] if using a NVIDIA graphics card.

Short descriptions of the alternatives are given in [8], and more information about these and other alternatives can be found in [11, 13, 16]. CUDA presents the user with a C language for direct application development on NVIDIA GPUs.

The development in this paper has been conducted using GLSL.

3. A GPU Particle Filter

3.1. Background. The *particle filter* (PF) [3] has proven to be a versatile tool applicable to surveillance [19], fusion of mixed sensors in wireless networks [20], cell phone localization [21], indoor localization [22], and *simultaneous localization and mapping* (SLAM) [23]. It extends to problems where nonlinearities may cause problems for traditional methods, such as the *Kalman filter* (KF) [24] or banks of KFs [25, 26]. The main drawback is its inherent computational complexity. This can, however, be handled by parallelization. The survey in [27] details a general PF framework for localization and tracking, and it also points out the importance of utilizing model structure using the *Rao-Blackwellized particle filter* (RBPF), also denoted *marginalized particle filter* (MPF) [28, 29]. The result is a

PF applied to a lowdimensional state vector, where a KF is attached to each particle enabling efficient and real-time implementations. Still, both the PF and RBPF are computer intensive algorithms requiring powerful processors.

3.2. The Particle Filter Algorithm. The general nonlinear filtering problem is to estimate the state, x_t, of a state-space system

$$\begin{aligned} x_{t+1} &= f(x_t, w_t), \\ y_t &= h(x_t) + e_t, \end{aligned} \tag{3}$$

where y_t is the measurement and $w_t \sim p_w(w_t)$ and $e_t \sim p_e(e_t)$ are the process and measurement noise, respectively. The function f describes the dynamics of the system, h the measurements, and p_w and p_e are *probability density functions* (PDFs) of the involved noise. For the important special case of linear-Gaussian dynamics and linear-Gaussian observations the Kalman filter [24, 30] solves the estimation problem in an optimal way. A more general solution is the *particle filter* (PF) [3, 31, 32] which approximately solves the Bayesian inference for the posterior state distribution [33] given by

$$\begin{aligned} p(x_{t+1} \mid \mathbb{Y}_t) &= \int p(x_{t+1} \mid x_t) p(x_t \mid \mathbb{Y}_t) dx_t, \\ p(x_t \mid \mathbb{Y}_t) &= \frac{p(y_t \mid x_t) p(x_t \mid \mathbb{Y}_{t-1})}{p(y_t \mid \mathbb{Y}_{t-1})}, \end{aligned} \tag{4}$$

where $\mathbb{Y}_t = \{y_i\}_{i=1}^t$ is the set of available measurements. The PF uses statistical methods to approximate the integrals. The basic PF algorithm is given in Algorithm 1.

To implement a parallel particle filter on a GPU there are several aspects of Algorithm 1 that require special attention. Resampling is the most challenging step to implement in parallel since all particles and their weights interact with each other. The main difficulties are cumulative summation, and selection and redistribution of particles. In the following sections, solutions suitable for parallel implementation are proposed for these tasks. Another important issue is how random numbers are generated, since this can consume a substantial part of the time spent in the particle filter. The remaining steps, likelihood evaluation as part of the measurement update and state propagation as part of the time update, are only briefly discussed since they are parallel in their nature.

The resulting parallel GPU implementation is illustrated in Figure 3. The steps are discussed in more detail in this section.

3.3. GPU PF: Random Number Generation. State-of-the-art graphics cards do not have sufficient support for random number generation for direct usage in a particle filter, since the statistical properties of the built-in generators are too poor.

The algorithm in this paper therefore relies on random numbers generated on the CPU to be passed to the GPU. This introduces substantial data transfer, as several random numbers per particle are needed in each iteration of the particle filter. Uploading data to the graphics card is rather quick, but performance is still lost. Furthermore, this makes generation of random numbers a $\mathcal{O}(N)$ operation instead of a $\mathcal{O}(1)$ operation, as would be the case if the generation was completely parallel.

Generating random numbers on the GPU suitable for use in Monte Carlo simulations is an ongoing research topic, see, for example, [34–36]. Implementing the random number generation in the GPU will not only reduce data transfer and allow for a standalone GPU implementation, an efficient parallel version will also improve the overall performance as the random number generation itself takes a considerable amount of time.

```
(1) Let $t := 0$, generate $N$ particles: $\{x_0^{(i)}\}_{i=1}^N \sim p(x_0)$.
(2) Measurement update: Compute the particle weights
      $\omega_t^{(i)} = p(y_t \mid x_t^{(i)}) / \sum_{j=1}^N p(y_t \mid x_t^{(j)})$.
(3) Resample:
      (a) Generate $N$ uniform random numbers
            $\{u_t^{(i)}\}_{i=1}^N \sim U(0,1)$.
      (b) Compute the cumulative weights:
            $c_t^{(i)} = \sum_{j=1}^i \omega_t^{(j)}$.
      (c) Generate $N$ new particles using $u_t^{(i)}$ and $c_t^{(i)}$:
            $\{x_{t+}^{(i)}\}_{i=1}^N$ where $\Pr(x_{t+}^{(i)} = x_t^{(j^{(i)})}) = \omega_t^{(j^{(i)})}$.
(4) Time update:
      (a) Generate process noise $\{w_t^{(i)}\}_{i=1}^N \sim p_w(w_t)$.
      (b) Simulate new particles $x_{t+1}^{(i)} = f(x_{t+}^{(i)}, w_t^{(i)})$.
(5) Let $t := t + 1$ and repeat from 2.
```

Algorithm 1: The Particle Filter [3].

3.4. GPU PF: Likelihood Evaluation and State Propagation. Both likelihood evaluation (as part of the measurement update) and state propagation (in the time update) of Algorithm 1, can be implemented straightforwardly in a parallel fashion since all particles are handled independently. Consequently, both operations can be performed in $\mathcal{O}(1)$ time with N parallel processors, that is, one processing element per particle. To solve new filtering problems, only these two functions have to be modified. As no parallelization issues need to be addressed, this is easily accomplished. In the presented GPU implementation the particles $x^{(i)}$ and the weights $\omega^{(i)}$ are stored in separate textures which are updated by the state propagation and the likelihood evaluation, respectively. One texture can only hold four-dimensional state vectors in a natural way, but using multiple rendering targets the state vectors can be extended when needed without any major changes to the code. The idea is then to store the state in several textures. For instance, with two textures to store the state, the state vector can grow to eight states. With the multitarget capability of modern graphics cards the changes needed are minimal.

When the measurement noise is lowdimensional (groups of at most 4 dependent dimensions to fit a lookup table in a

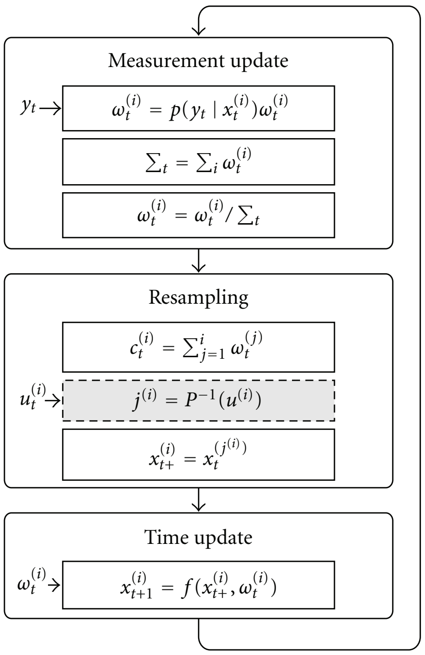
Measurement update
y_t
$\omega_t^{(i)} = p(y_t \mid x_t^{(i)})\omega_t^{(i)}$
$\sum_t = \sum_i \omega_t^{(i)}$
$\omega_t^{(i)} = \omega_t^{(i)}/\sum_t$
Resampling
$c_t^{(i)} = \sum_{j=1}^{i} \omega_t^{(j)}$
$u_t^{(i)}$
$j^{(i)} = P^{-1}(u^{(i)})$
$x_{t+}^{(i)} = x_t^{(j(i))}$
Time update
$\omega_t^{(i)}$
$x_{t+1}^{(i)} = f(x_{t+}^{(i)}, \omega_t^{(i)})$

FIGURE 3: GPU PF algorithm. The outer boxes make up the CPU program starting the inner boxes on the GPU in correct order. The figure also indicates what is fed to the GPU; remaining data is generated on it.

```
uniform    vec2 y;
uniform    sampler2D x, w, pdf;
uniform    mat2   sqrtSigmainv;
const   vec2   S1 = vec2(1., 0);
const   vec2   S2 = vec2(-1., 0);
void   main(void)
{
vec2   xtmp=texture2D(x, g1_TexCoord[0]. st ). xy;
vec2   e = y-vec2(distance(xtmp, S1), distance (xtmp, S2));
e=sqrtSigmainv * e + vec2(.5,.5);
g1_FragColor.x = texture2D(pdf, e).x
*    texture2D(w, g1_Texcoord[0].st).x;
}
```

LISTING 1: GLSL coded fragment shader: measurement update.

texture) the likelihood computations can be replaced by fast texture lookups utilizing the fast texture interpolation. The result is not as exact as if the likelihood was computed the regular way, but the increase in speed is often considerable.

Furthermore, as discussed above, the state propagation uses externally generated process noise, but it would also be possible to generate the random numbers on the GPU.

Example (Shader program). To exemplify GLSL source code, Listing 1 contains the code needed for a measurement update in the range-only measurement example in Section 4.

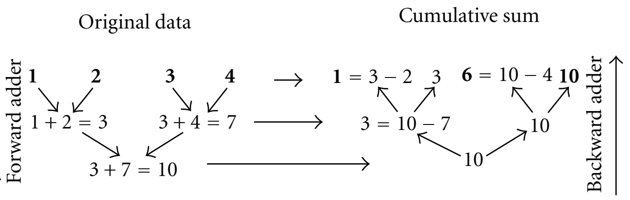

FIGURE 4: A parallel implementation of cumulative sum generation of the numbers 1, 2, 3, and 4. First the sum, 10, is calculated using a forward adder tree. Then the partial summation results are used by the backward adder to construct the cumulative sum; 1, 3, 6, and 10.

The code is very similar to C code, and is executed once for each particle, that is, fragment. To run the program a rectangle is fed as vertices to the graphics card. The size of the rectangle is chosen such that there will be exactly one fragment per particle, and that way the code is executed once for every particle.

The keyword **uniform** indicates that the following variable is set by the API before the program is executed. The variable y is hence a two-component vector, **vec2**, with the measurement, and S_1 and S_2 contain the locations of the sensors. Variables of the type **sampler2D** are pointers to specific texture units, and hence x and w point out particles and weights, respectively, and pdf the location of the lookup table for the measurement likelihood.

The first line of code makes a texture lookup and retrieves the state, stored as the two first components of the vector (color data) as indicated by the xy suffix. The next line computes the difference between the measurement and the predicted measurement, before the error is scaled and shifted to allow for a quick texture look up. The final line writes the new weight to the output.

3.5. GPU PF: Summation. Summation is part of the weight normalization (as the last step of the measurement update) and the cumulative weight calculation (during resampling) of Algorithm 1. A cumulative sum can be implemented using a multipass scheme, where an adder tree is run forward and then backward, as illustrated in Figure 4. This multipass scheme is a standard method for parallelizing seemingly sequential algorithms based on the scatter and gather principles. In [11], these concepts are described in the GPU setting. In the forward pass partial sums are created that are used in the backward pass to compute the missing partial sums to complete the cumulative sum. The resulting algorithm is $\mathcal{O}(\log N)$ in time given N parallel processors and N particles.

3.6. GPU PF: Resampling. To prevent sample impoverishment, the resampling step of Algorithm 1 replaces unlikely particles with likelier ones. This is done by drawing a new set of particles $\{x_+^{(i)}\}$ with replacement from the original particles $\{x^{(i)}\}$ in such a way that $\Pr(x_+^{(i)} = x^{(j)}) = \omega^{(j)}$. Standard resampling algorithms [31, 37] select new particles

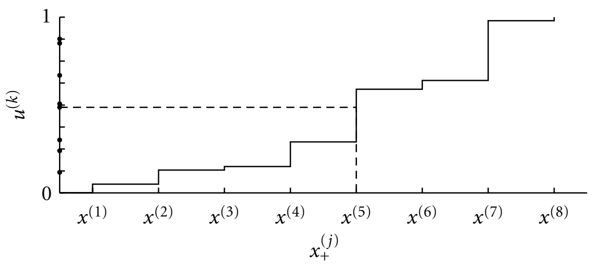

FIGURE 5: Particle selection by comparing uniform random numbers (•) to the cumulative sum of particle weights (–).

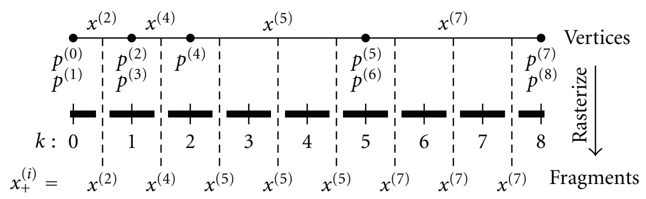

$x^{(2)}$ $x^{(4)}$ $x^{(5)}$ $x^{(7)}$
Vertices
$p^{(0)}$ $p^{(1)}$ $p^{(2)}$ $p^{(3)}$ $p^{(4)}$ $p^{(5)}$ $p^{(6)}$ $p^{(7)}$ $p^{(8)}$
Rasterize
k: 0 1 2 3 4 5 6 7 8
$x_+^{(i)}$ = $x^{(2)}$ $x^{(4)}$ $x^{(5)}$ $x^{(5)}$ $x^{(5)}$ $x^{(7)}$ $x^{(7)}$ $x^{(7)}$
Fragments

FIGURE 6: Particle selection on the GPU. The line segments are made up by the points $N^{(i-1)}$ and $N^{(i)}$, which define a line where every segment represents a particle. Some line segments have length 0, that is, no particle should be selected from them. The rasterizer creates particles x according to the length of the line segments. The line segments in this figure match the situation in Figure 5.

using uniformly distributed random numbers as input to the inverse CDF given by the particle weights

$$x_{t+}^{(i)} = x_t^{(j^{(i)})}, \quad \text{with } j^{(i)} = P^{-1}\left(u^{(j^{(i)})}\right), \tag{5}$$

where P is the CDF given by the particle weights.

The idea for the GPU implementation is to use the rasterizer to do stratified resampling. Stratified resampling is especially suitable for parallel implementation because it produces ordered random numbers, and guarantees that if the interval $(0, 1]$ is divided into N intervals, there will be exactly one random number in each subinterval of length N^{-1}. Selecting which particles to keep is done by drawing a line. The line consists of one line segment for each particle in the original set, indicated by its color, and where the length of the segments indicate how many times the particles should be replicated. With appropriate segments, the rastering will create evenly spaced fragments from the line, hence giving more fragments from long line segments and consequently more particles of likelier particles. The properties of the stratified resampling are perfect for this. They make it possible to compute how many particles have been selected once a certain point in the original distribution was selected. The expression for this is

$$N^{(i)} = \left\lceil Nc^{(i)} - u^{(\lfloor Nc^{(i)} \rfloor)} \right\rceil, \tag{6}$$

where N is the total number of particles, $c^{(i)} = \sum_{j=1}^{i} \omega^{(j)}$ is the ith cumulative weight sum, and $N^{(i)}$ the number of particles selected when reaching the ith particle in the

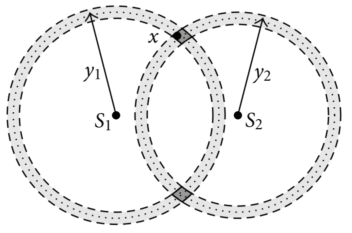

FIGURE 7: A range-only sensor system, with 2D-position sensors in S_1 and S_2 with indicated range resolution.

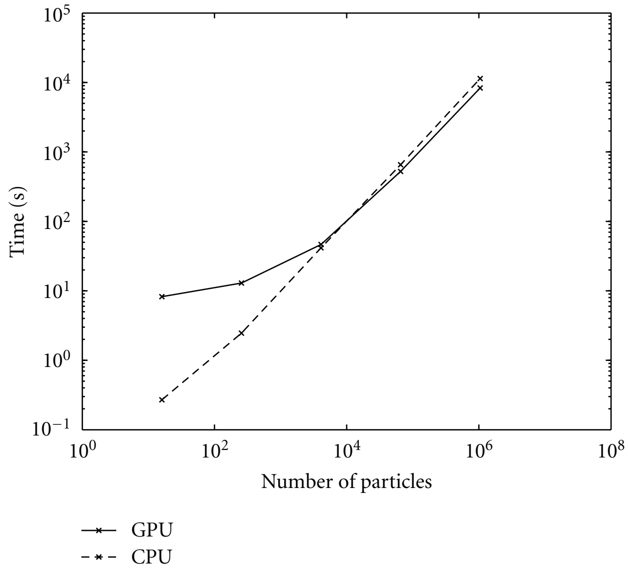

FIGURE 8: Comparison of time used for GPU and CPU.

original set. The expression for stratified resampling is vital for parallelizing the resampling step, and hence to make a GPU implementation possible. By drawing the line segment for particle i from $N^{(i-1)}$ to $N^{(i)}$, with $N^{(0)} = 0$, the particles that should survive the resampling step correspond to a line segment as long as the number of copies there should be in the new set. Particles which should not be selected get line segments of zero length. Rastering with unit length between the fragments will therefore produce the correct set of resampled particles, as illustrated in Figure 6 for the weights in Figure 5. The computational complexity of this is $\mathcal{O}(1)$ with N parallel processors, as the vertex positions can be calculated independently. Unfortunately, the used generation of GPUs has a maximal texture size limiting the number of particles that can be resampled as a single unit. To solve this, multiple subsets of particles are simultaneously being resampled and then redistributed into different sets, similarly to what is described in [38]. This modification of the resampling step does not seem to significantly affect the performance of the particle filter as a whole.

3.7. GPU PF: Computational Complexity. From the descriptions of the different steps of the particle filter algorithm it is clear that the resampling step is the bottleneck that gives the

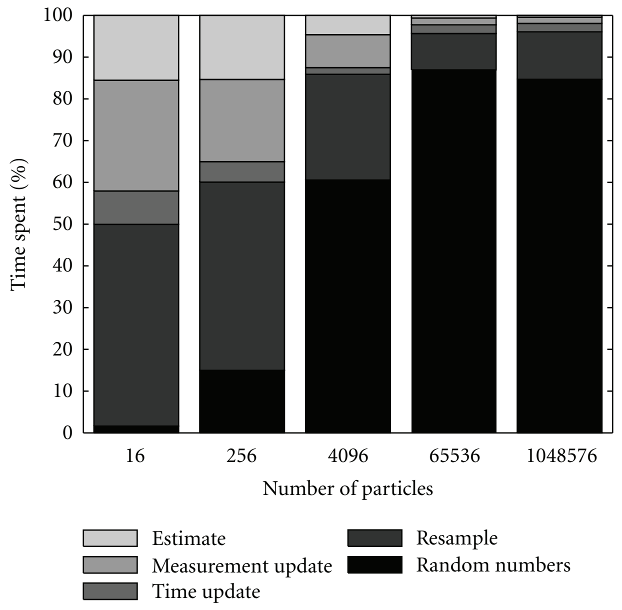

(a) GPU

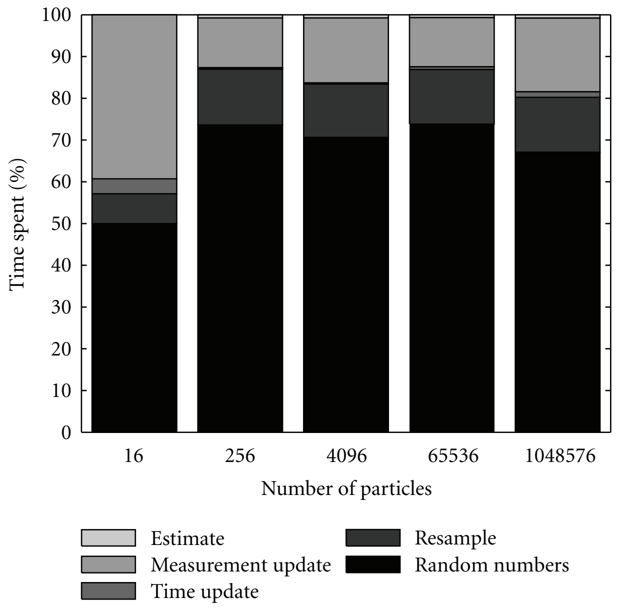

(b) CPU

FIGURE 9: Comparison of the relative time spent in the different steps particle filter, in the GPU and CPU implementation, respectively.

time complexity of the algorithm, $\mathcal{O}(\log N)$ for the parallel algorithm compared to $\mathcal{O}(N)$ for a sequential algorithm.

The analysis of the algorithm complexity above assumes that there are as many parallel processors as there are particles in the particle filter, that is, N parallel elements. Today this is a bit too optimistic, there are hundreds of parallel pipelines in a modern GPU, hence much less than the typical number of particles. However, the number of parallel units is constantly increasing.

Especially the cumulative sum suffers from a low degree of parallelization. With full parallelization the time complexity of the operation is $\mathcal{O}(\log N)$ whereas a sequential algorithm is $\mathcal{O}(N)$, however the parallel implementation uses $\mathcal{O}(2N)$ operations in total. That is, the parallel implementation uses about twice as many operations as the sequential implementation. This is the price to pay for the parallelization, but is of less interest as the extra operations are shared between many processors. As a result, with few pipelines and many particles the parallel implementation will have the same complexity as the sequential one, roughly $\mathcal{O}(N/M)$ where M is the number of processors.

4. Simulations

Consider the following range-only application as depicted in Figure 7. The following state-space model represents the 2D-position

$$x_{t+1} = x_t + w_t,$$
$$y_t = h(x_t) + e_t = \begin{pmatrix} \|x_t - S_1\|_2 \\ \|x_t - S_2\|_2 \end{pmatrix} + e_t, \tag{7}$$

TABLE 2: Hardware used for the evaluation.

GPU		CPU	
Model:	NVIDIA GeFORCE 7900 GTX	Model:	Intel Xeon 5130
Driver:	2.1.2 NVIDIA 169.09	Clock speed:	2.0 GHz
Bus:	PCI Express, 14.4 GB/s	Memory:	2.0 GB
Clock speed:	650 MHz	OS:	CentOS 5.1,
Processors:	8/24 (vertex/fragment)		64 bit (Linux)

where S_1 and S_2 are sensor locations and x_t contains the 2D-position of the object. This could be seen as a central node in a small sensor network of two nodes, which easily can be expanded to more nodes.

To verify the correctness of the implementation a particle filter, using the exact same resampling scheme, has been designed for the GPU and the CPU. The resulting filters give practically identical results, though minor differences exist due to the less sophisticated rounding unit available in the GPU and the trick in computing the measurement likelihood. Furthermore, the performance of the filters is comparable to what has been achieved previously for this problem.

To evaluate the complexity gain obtained from using the parallel GPU implementation, the GPU and the CPU implementations of the particle filter were run and timed. Information about the hardware used for this is gathered in Table 2. Figure 8 gives the total time for running the filter for 100 time steps repeated 100 times for a set of different numbers of particles ranging from $2^4 = 16$ to $2^{20} \approx 10^6$.

(Note that 16 particles are not enough for this problem, nor is as many as 10^6 needed. However, the large range shows the complexity better.)

Some observations: for few particles the overhead from initializing and using the GPU is large and hence the CPU implementation is the fastest. With more work optimizing the parallel implementation the gap could be reduced. The CPU complexity follows a linear trend, whereas at first the GPU time hardly increases when using more particles; parallelization pays off. For even more particles there are not enough parallel processing units available and the complexity becomes linear, but the GPU implementation is still faster than the CPU. Note that the particle selection is performed on 8 processors and the other steps on 24, see Table 2, and hence that the degree of parallelization is not very high with many particles.

A further analysis of the time spent in the GPU implementation shows which parts are the most time consuming, see Figure 9. The main cost in the GPU implementation quickly becomes the random number generation (performed on the CPU), which shows that if that step can be parallelized there is much to gain in performance. For both CPU and GPU the time update step is almost negligible, which is an effect of the simple dynamic model. The GPU would have gained from a computationally expensive time update step, where the parallelization would have paied off better. To produce an estimate from the GPU is relatively more expensive than it is with the CPU. For the CPU all steps are $\mathcal{O}(N)$ whereas for the GPU the estimate is $\mathcal{O}(\log N)$ where both the measurement update and the time update steps are $\mathcal{O}(1)$. Not counting the random number generation, the major part of the time is spent on resampling in the GPU, whereas the measurement update is a much more prominent step in the CPU implementation. One reason is the implemented hardware texture lookups for the measurement likelihood in the GPU.

5. Conclusions

In this paper, the first complete parallel general particle filter implementation in literature on a GPU is described. Using simulations, the parallel GPU implementation is shown to outperform a CPU implementation when it comes to computation speed for many particles while maintaining the same filter quality. As the number of pipelines steadily increases, and can be expected to match the number of particles needed for some low-dimensional problems, the GPU is an interesting alternative platform for PF implementations. The techniques and solutions used in deriving the implementation can also be used to implement particle filters on other similar parallel architectures.

References

[1] M. D. Hill and M. R. Marty, "Amdahl's law in the multicore era," *Computer*, vol. 41, no. 7, pp. 33–38, 2008.

[2] S. Borkar, "Thousand core chips: a technology perspective," in *Proceedings of the 44th ACM/IEEE Design Automation Conference (DAC'07)*, pp. 746–749, June 2007.

[3] N. J. Gordon, D. J. Salmond, and A. F. M. Smith, "Novel approach to nonlinear/non-Gaussian Bayesian state estimation," *IEE Proceedings, Part F*, vol. 140, no. 2, pp. 107–113, 1993.

[4] F. Gustafsson, "Particle filter theory and practice with positioning applications," to appear in *IEEE Aerospace and Electronic Systems*, magazine vol. 25, no. 7 july 2010 part 2: tutorials.

[5] A. S. Montemayor, J. J. Pantrigo, A. Sánchez, and F. Fernández, "Particle filter on GPUs for real time tracking," in *Proceedings of the International Conference on Computer Graphics and Interactive Techniques (SIGGRAPH '04)*, p. 94, Los Angeles, Calif, USA, August 2004.

[6] S. Maskell, B. Alun-Jones, and M. Macleod, "A single instruction multiple data particle filter," in *Proceedings of Nonlinear Statistical Signal Processing Workshop (NSSPW '06)*, Cambridge, UK, September 2006.

[7] G. Hendeby, J. D. Hol, R. Karlsson, and F. Gustafsson, "A graphics processing unit implementation of the particle filter," in *Proceedings of the 15th European Statistical Signal Processing Conference (EUSIPCO '07)*, pp. 1639–1643, Poznań, Poland, September 2007.

[8] G. Hendeby, *Performance and implementation aspects of nonlinear filtering*, Ph.D. thesis, Linköping Studies in Science and Technology, March 2008.

[9] "MAGMA," 2009, http://icl.cs.utk.edu/magma/.

[10] "NVIDIA CUDA applications browser," 2009, http://www.nvidia.com/content/cudazone/CUDABrowser/assets/data/applications.xml.

[11] M. Pharr, Ed., *GPU Gems 2. Programming Techniques for High-Performance Graphics and General-Purpose Computation*, Addison-Wesley, Reading, Mass, USA, 2005.

[12] M. D. Mccool, "Signal processing and general-purpose computing and GPUs," *IEEE Signal Processing Magazine*, vol. 24, no. 3, pp. 110–115, 2007.

[13] "GPGPU programming," 2006, http://www.gpgpu.org/.

[14] D. Shreiner, M. Woo, J. Neider, and T. Davis, *OpenGL Programming Language. The Official Guide to learning OpenGL, Version 2*, Addison-Wesley, Reading, Mass, USA, 5th edition, 2005.

[15] R. J. Rost, *OpenGL Shading Language*, Addison-Wesley, Reading, Mass, USA, 2nd edition, 2006.

[16] "NVIDIA developer," 2006, http://developer.nvidia.com/.

[17] M. Corporation, "High-level shader language. In DirectX 9.0 graphics," 2008, http://msdn.microsoft.com/directx.

[18] "CUDA zone—learn about CUDA," 2009, http://www.nvidia.com/object/cuda_what_is.html.

[19] Y. Zou and K. Chakrabarty, "Distributed mobility management for target tracking in mobile sensor networks," *IEEE Transactions on Mobile Computing*, vol. 6, no. 8, pp. 872–887, 2007.

[20] R. Huang and G. V. Záruba, "Incorporating data from multiple sensors for localizing nodes in mobile ad hoc networks," *IEEE Transactions on Mobile Computing*, vol. 6, no. 9, pp. 1090–1104, 2007.

[21] L. Mihaylova, D. Angelova, S. Honary, D. R. Bull, C. N. Canagarajah, and B. Ristic, "Mobility tracking in cellular networks using particle filtering," *IEEE Transactions on Wireless Communications*, vol. 6, no. 10, pp. 3589–3599, 2007.

[22] X. Chai and Q. Yang, "Reducing the calibration effort for probabilistic indoor location estimation," *IEEE Transactions on Mobile Computing*, vol. 6, no. 6, pp. 649–662, 2007.

[23] M. Montemerlo, S. Thrun, D. Koller, and B. Wegbreit, "FastSLAM 2.0: an improved particle filtering algorithm for

simultaneous localization and mapping that provably converges," in *Proceedings of the 18th International Joint Conference on Artificial Intelligence*, pp. 1151–1157, Acapulco, Mexico, August 2003.

[24] R. E. Kalman, "A new approach to linear filtering and prediction problems," *Journal of Basic Engineering*, vol. 82, pp. 35–45, 1960.

[25] Y. Bar-Shalom and X. R. Li, *Estimation and Tracking: Principles, Techniques, and Software*, Artech House, Boston, Mass, USA, 1993.

[26] B. D. O. Anderson and J. B. Moore, *Optimal Filtering*, Prentice-Hall, Englewood Cliffs, NJ, USA, 1979.

[27] F. Gustafsson, F. Gunnarsson, N. Bergman et al., "Particle filters for positioning, navigation, and tracking," *IEEE Transactions on Signal Processing*, vol. 50, no. 2, pp. 425–437, 2002.

[28] R. Chen and J. S. Liu, "Mixture Kalman filters," *Journal of the Royal Statistical Society. Series B*, vol. 62, no. 3, pp. 493–508, 2000.

[29] T. Schön, F. Gustafsson, and P.-J. Nordlund, "Marginalized particle filters for mixed linear/nonlinear state-space models," *IEEE Transactions on Signal Processing*, vol. 53, no. 7, pp. 2279–2289, 2005.

[30] T. Kailath, A. H. Sayed, and B. Hassibi, *Linear Estimation*, Prentice-Hall, Englewood Cliffs, NJ, USA, 2000.

[31] A. Doucet, N. de Freitas, and N. Gordon, Eds., *Sequential Monte Carlo Methods in Practice*, Statistics for Engineering and Information Science, Springer, New York, NY, USA, 2001.

[32] B. Ristic, S. Arulampalam, and N. Gordon, *Beyond the Kalman Filter: Particle Filters for Tracking Applications*, Artech House, Boston, Mass, USA, 2004.

[33] A. H. Jazwinski, *Stochastic Processes and Filtering Theory*, vol. 64 of *Mathematics in Science and Engineering*, Academic Press, New York, NY, USA, 1970.

[34] A. De Matteis and S. Pagnutti, "Parallelization of random number generators and long-range correlations," *Numerische Mathematik*, vol. 53, no. 5, pp. 595–608, 1988.

[35] C. J. K. Tan, "The PLFG parallel pseudo-random number generator," *Future Generation Computer Systems*, vol. 18, no. 5, pp. 693–698, 2002.

[36] M. Sussman, W. Crutchfield, and M. Papakipos, "Pseudo-random number generation on the GPU," in *Proceedings of the 21st ACM SIGGRAPH/Eurographics Symposium Graphics Hardware*, pp. 87–94, Vienna, Austria, September 2006.

[37] G. Kitagawa, "Monte Carlo filter and smoother for non-Gaussian nonlinear state space models," *Journal of Computational and Graphical Statistics*, vol. 5, no. 1, pp. 1–25, 1996.

[38] M. Bolić, P. M. Djurić, and S. Hong, "Resampling algorithms and architectures for distributed particle filters," *IEEE Transactions on Signal Processing*, vol. 53, no. 7, pp. 2442–2450, 2005.